

## Visible emission from Er-doped GaN grown by solid source molecular beam epitaxy

A. J. Steckl<sup>a)</sup> and R. Birkhahn

Nanoelectronics Laboratory, University of Cincinnati, Cincinnati, Ohio 45221-0030

(Received 3 June 1998; accepted for publication 22 July 1998)

Visible light emission has been obtained from Er-doped GaN thin films. The GaN was grown by molecular beam epitaxy on sapphire substrates using solid sources (for Ga, Al, and Er) and a plasma gas source for N<sub>2</sub>. Above GaN band-gap photoexcitation resulted in strong green emission. The emission spectrum consists of two narrow green lines at 537 and 558 nm and a broad peak at light blue wavelengths (480–510 nm). The narrow lines have been identified as Er transitions from the <sup>2</sup>H<sub>11/2</sub> and <sup>4</sup>S<sub>3/2</sub> levels to the <sup>4</sup>I<sub>15/2</sub> ground state. The intensity of the 558 nm emission decreases with increasing temperature, while the intensity of the 537 nm line actually peaks at ~300 K. This effect is explained based on the thermalization of electrons between the two closely spaced energy levels.

© 1998 American Institute of Physics. [S0003-6951(98)03438-X]

While great progress<sup>1</sup> is being made in enhancing the emission intensity of Er-doped Si, it still experiences significant loss in luminescence efficiency at room temperature compared to low temperature. This thermal quenching was shown<sup>2</sup> by Favennec *et al.* to decrease with the band-gap energy of the semiconductor. Examples of rare earth (RE)-doped wide band-gap semiconductors (WBGs) which have been reported include GaP,<sup>3</sup> SiC,<sup>4</sup> and III–V compounds.<sup>5</sup> Advantages of WBGs over other semiconductors and glasses also include chemical stability, carrier generation (to excite the RE), and physical stability over a wide temperature range. The III–N semiconducting compounds are of particular interest because of their direct band gap and high level of optical activity even under conditions of rather high defect density, which would quench emission in other smaller-gap III–V and wide-gap II–VI compounds. Laser diodes fabricated using GaN-based structures are rapidly reaching the commercialization stage.

The doping of III nitrides (GaN, AlN) with Er by molecular beam epitaxy (MBE) and metalorganic chemical vapor deposition (MOCVD) both during growth and post growth by ion implantation has been recently reported.<sup>6–16</sup> The successful *in situ* incorporation<sup>12,15,16</sup> of Er into AlN and GaN by MBE and its infrared (IR) emission characteristics have been reported. None of the papers in the literature report emission in the visible range from Er-doped III-nitrides.

We have grown Er-doped GaN films in a Riber MBE-32 system directly on *c*-axis sapphire substrates. Solid sources were employed to supply the Ga (7 N purity), Al (6 N), and Er (3 N) fluxes, while an SVTA Corp. rf plasma source was used to generate atomic nitrogen. The substrate was initially nitrided at 750 °C for 30 min at 400 W rf power with a N<sub>2</sub> flow rate of 1.5 sccm, corresponding to a chamber pressure of mid-10<sup>-5</sup> Torr. An AlN buffer layer was grown at 550 °C for 10 min with an Al beam pressure of 2.3 × 10<sup>-8</sup> Torr (cell temperature of 970 °C). Growth of the Er-doped GaN proceeded at 750 °C for 3 h with a constant Ga beam pressure of

8.2 × 10<sup>-7</sup> Torr (cell temperature of 922 °C). The Er cell temperature was varied from 950 to 1100 °C. The resulting GaN film thickness was nominally 2.4 μm giving a growth rate of 0.8 μm/h, as measured by scanning electron microscopy (SEM) and transmission optical spectroscopy.

Photoluminescence (PL) characterization was performed with two excitation sources: (a) above the GaN band gap—He–Cd laser at 325 nm (4–8 mW on the sample); (b) below the GaN band gap—Ar laser at 488 nm (25–30 mW). The PL signal was analyzed by a 0.3 m Acton Research spectrometer outfitted with a photomultiplier for ultraviolet (UV)-visible wavelengths (350–600 nm) and an InGaAs detector for infrared (1.5 μm) measurements. The PL signal of the Er-doped GaN samples was obtained over the 88–400 K temperature range.

Above band-gap excitation (He–Cd laser) resulted in light green emission from the Er-doped GaN films, visible with the naked eye. The room temperature PL at visible wavelengths is shown in Fig. 1 for a GaN film grown on sapphire at 750 °C with the Er cell at a temperature of

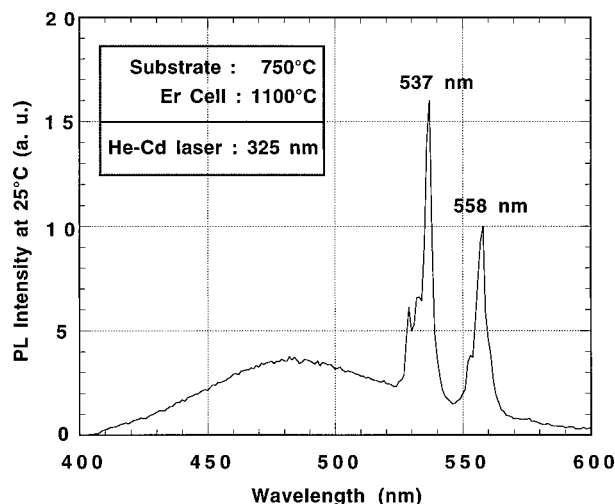


FIG. 1. Visible PL spectrum of Er-doped GaN film grown on sapphire at 950 °C with an Er cell temperature of 1100 °C. The PL is performed at room temperature with the He–Cd laser line at 325 nm.

<sup>a)</sup>Electronic mail: a.steckl@uc.edu

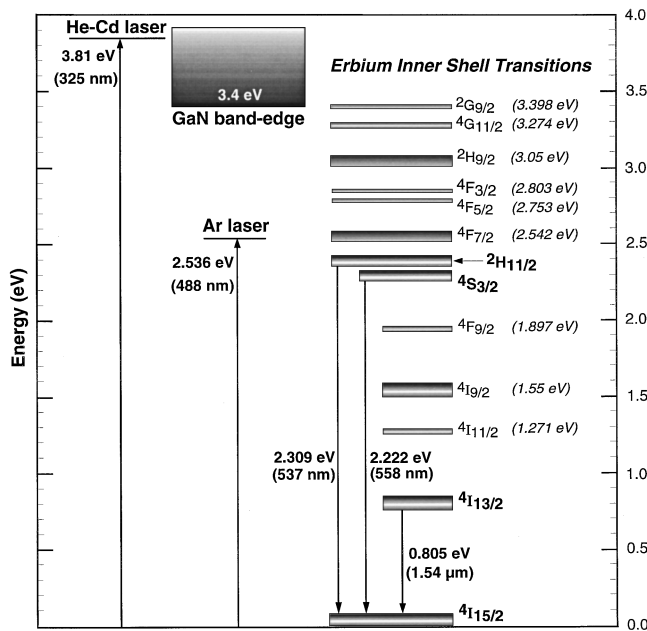


FIG. 2. Relevant energy levels in the PL of GaN:Er films: excitation laser photon energies, GaN conduction band edge and Er 4f energy levels.

1100 °C. Two major emission multiplets are observed in the green wavelength region with the strongest lines at 537 and 558 nm. A broad emission region is also present, peaking in the light blue at 480 nm. The yellow band typically observed at ~540–550 nm in GaN PL is absent. Interestingly, utilizing below band-gap excitation (Ar laser) we did not observe the green emission. While this letter is concerned with visible emission from GaN:Er, the near IR emission at 1.5  $\mu\text{m}$  is also of great practical importance. Both above band-gap and below-gap excitation resulted in near-IR emission.

The relationship between the excitation photon energy and the PL emitted photon energy can be more easily discussed by referring to Fig. 2, where the Er inner shell transition energies up to the GaN band-gap energy (3.4 eV) are shown along with the pump laser photon energies. The transition energy (shown in parentheses) and approximate width of the Er levels are based on the emission spectrum of the free trivalent  $\text{Er}^{3+}$  ion (see, for example, Dieke and Crosswhite<sup>17</sup>). The green emission lines are produced by  ${}^2H_{11/2}$  and  ${}^4S_{3/2}$  transitions to the  ${}^4I_{15/2}$  ground state. The 1.5  $\mu\text{m}$  emission is generated by transitions from the  ${}^4I_{13/2}$  state to the same ground state. The energy values associated with these three transitions (shown in bold) are based on the PL emission spectra from our GaN:Er films. Photopumping with the 3.8 eV photons of the He–Cd laser produces strong promotion of electrons into the GaN conduction band because of the high absorption coefficient at above band-gap wavelengths. A certain fraction of these excited carriers lose their energy through radiative recombination accompanied by GaN band-edge emission. However, many excited electrons experience nonradiative phonon transitions until they reach the various inner shell energy levels of the Er atoms where they can transfer their energy. While many of the Er transitions are in principle parity forbidden, the Stark splitting of these levels, which occurs because of interaction with the host material, results in some of them becoming allowed transitions. In RE-doped glasses, many of these levels show

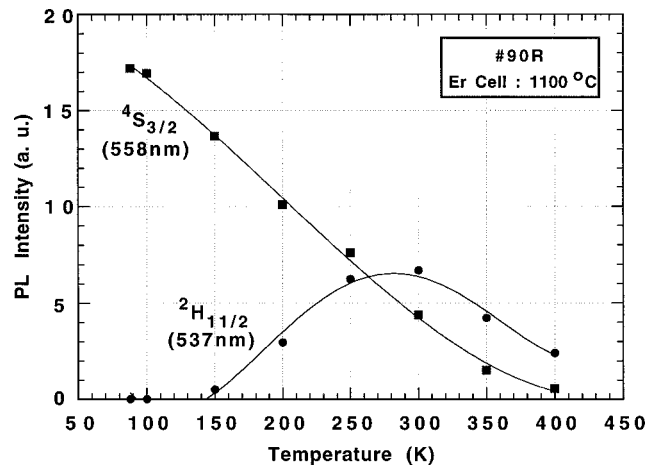


FIG. 3. The temperature dependence of the green PL lines from a GaN:Er film.

radiative transitions. However, in RE-doped semiconductors only the transition from the lowest-lying excited state (the  ${}^4I_{13/2}$  level in the case of Er) has been generally reported. In our GaN:Er films we have observed for the first time strong emission from upper excited levels ( ${}^2H_{11/2}$  and  ${}^4S_{3/2}$ ) when photopumping with the He–Cd laser. It is interesting to point out that photons from the 488 Ar laser line, which do not produce this visible green emission, have sufficient energy (~2.54 eV) to be absorbed by these Er levels. Utilizing above GaN band-gap excitation is a more efficient process because of the combination of strong photogeneration of excited electrons and efficient energy transfer to Er ions.

The temperature dependence of the PL intensity of the  ${}^2H_{11/2}$  and  ${}^4S_{3/2}$  lines is shown in Fig. 3 for the GaN:Er film grown with an Er cell temperature of 1100 °C. It is important to note that the intensity of the  ${}^4S_{3/2}$  line decreases monotonically with increasing temperature, while the  ${}^2H_{11/2}$  line has a maximum at around 300 K. The two curves actually cross at ~250 K, with the  ${}^2H_{11/2}$  line being consistently stronger than the  ${}^4S_{3/2}$  line at higher temperatures. The most likely explanation for the opposite temperature dependence between the two closely spaced electronic states is that electrons are thermally equilibrated between the two levels at temperatures below 300 K. Under thermalization conditions,

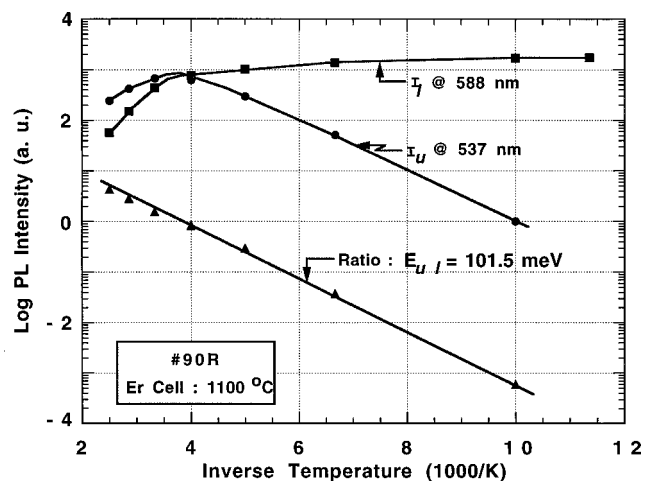


FIG. 4. Ratio of PL intensity from the  ${}^2H_{11/2}$  and  ${}^4S_{3/2}$  lines as a function of reciprocal measurement temperature.

as we decrease the temperature from 300 to 88 K, the PL intensity from the upper  ${}^2H_{11/2}$  level is reduced as it increasingly feeds electrons to the lower  ${}^4S_{3/2}$  level, whose intensity increases as we reduce the temperature. Above 300 K, the intensity of both levels decreases with increasing temperature, indicating that the supply of electrons to the  ${}^2H_{11/2}$  and  ${}^4S_{3/2}$  states is being reduced by other (nonradiative) transition paths.

The thermalization effect can be further discussed by considering the Arrhenius-type plot shown in Fig. 4 for the emission intensities from the  ${}^2H_{11/2}$  and  ${}^4S_{3/2}$  states, along with their ratio. The ratio of the emission intensities of the  ${}^2H_{11/2}$  and  ${}^4S_{3/2}$  states can be described (Yokokawa *et al.*<sup>18</sup>) by the following relation:

$$\frac{I_u}{I_l} = A e^{-E_{ul}/k_B T}, \quad (1)$$

where  $I_u$  and  $I_l$  are the luminescence intensities of the upper and lower levels,  $E_{ul}$  is their energy gap,  $A$  is a constant containing the degeneracies and spontaneous emission rates of the two levels, and  $k_B$  is the Boltzmann constant. The  $E_{ul}$  value calculated from these data is 101.5 meV. This is comparable to the value of 87.2 meV obtained from the energy difference between the two PL peaks. It is interesting to also compare our results to those obtained by Yokokawa *et al.*<sup>18</sup> for Er-doped ZBLAN (containing Zr, Ba, Al, and Na) fluoride glass. They reported a very similar thermalization effect between the  ${}^2H_{11/2}$  and  ${}^4S_{3/2}$  states with a value of  $E_{ul}$  of  $\sim 110$  meV and an energy difference between the two PL peaks of  $\sim 71$  meV. We can conclude that, at least in this respect, the behavior of Er in GaN and in fluoride glass is substantially the same.

In summary, we have reported the optical characteristics of Er-doped GaN grown by solid source MBE on sapphire. We have observed for the first time visible emission from Er in GaN. The fortuitous temperature dependence of the  ${}^2H_{11/2}$  level, which peaks at room temperature, has significant implications for future device applications of GaN:Er.

This work was supported by a BMDO/ARO contract (L. Lome and J. Zavada) and an ARO AASERT grant. The authors would like to acknowledge many technical discussions and the support and encouragement of J. Zavada. Equipment support was provided by an ARO URI grant and the Ohio Materials Network.

- <sup>1</sup>S. Coffa, G. Franzo, and F. Priolo, *MRS Bull.* **23**, 25 (1998).
- <sup>2</sup>P. N. Favanne, H. L'Haridon, M. Salvi, D. Moutonnet, and Y. Le Guillou, *Electron. Lett.* **25**, 718 (1989).
- <sup>3</sup>A. J. Neuhalfen and B. W. Wessels, *Appl. Phys. Lett.* **60**, 2657 (1992).
- <sup>4</sup>W. J. Choyke, R. P. Devaty, L. L. Clemen, M. Yoganathan, G. Pensl, and Ch. Hassler, *Appl. Phys. Lett.* **65**, 1668 (1994).
- <sup>5</sup>J. M. Zavada and D. Zhang, *Solid-State Electron.* **38**, 1285 (1995).
- <sup>6</sup>J. D. MacKenzie, C. R. Abernathy, S. J. Pearton, U. Hömmerich, X. Wu, R. N. Schwartz, R. G. Wilson, and J. M. Zavada, *Appl. Phys. Lett.* **69**, 2083 (1996).
- <sup>7</sup>J. T. Torvik, R. J. Feuerstein, J. I. Pankove, C. H. Qiu, and F. Namavar, *Appl. Phys. Lett.* **69**, 2098 (1996).
- <sup>8</sup>X. Wu, U. Hömmerich, J. D. MacKenzie, C. R. Abernathy, S. J. Pearton, R. N. Schwartz, R. G. Wilson, and J. M. Zavada, *Appl. Phys. Lett.* **70**, 2126 (1997).
- <sup>9</sup>S. Kim, S. J. Rhee, D. A. Turnbull, E. E. Reuter, X. Li, J. J. Coleman, and S. G. Bishop, *Appl. Phys. Lett.* **71**, 231 (1997).
- <sup>10</sup>M. Thaik, U. Hömmerich, R. N. Schwartz, R. G. Wilson, and J. M. Zavada, *Appl. Phys. Lett.* **71**, 2641 (1997).
- <sup>11</sup>S. Kim, S. J. Rhee, D. A. Turnbull, X. Li, J. J. Coleman, S. G. Bishop, and P. B. Klein, *Appl. Phys. Lett.* **71**, 2662 (1997).
- <sup>12</sup>J. D. MacKenzie, C. R. Abernathy, S. J. Pearton, S. M. Donovan, U. Hömmerich, M. Thaik, X. Wu, F. Ren, R. G. Wilson, and J. M. Zavada, *Mater. Res. Soc. Symp. Proc.* **468**, 123 (1997).
- <sup>13</sup>S. Kim, S. J. Rhee, D. A. Turnbull, X. Li, J. J. Coleman, and S. G. Bishop, *Mater. Res. Soc. Symp. Proc.* **468**, 131 (1997).
- <sup>14</sup>J. T. Torvik, C. H. Qiu, R. J. Feuerstein, J. I. Pankove, and F. Namavar, *J. Appl. Phys.* **81**, 6343 (1997).
- <sup>15</sup>J. D. MacKenzie, C. R. Abernathy, S. J. Pearton, U. Hömmerich, X. Wu, R. N. Schwartz, R. G. Wilson, and J. M. Zavada, *J. Cryst. Growth* **175/176**, 84 (1997).
- <sup>16</sup>D. M. Hansen, R. Zhang, N. R. Perkins, S. Safvi, L. Zhang, K. L. Bray, and T. F. Keuch, *Appl. Phys. Lett.* **72**, 1244 (1998).
- <sup>17</sup>G. H. Dieke and H. M. Crosswhite, *Appl. Opt.* **2**, 675 (1963).
- <sup>18</sup>T. Yokokawa, H. Inokuma, Y. Ohki, H. Nishikawa, and Y. Hama, *J. Appl. Phys.* **77**, 4013 (1995).